JOURNAL OF MATERIALS SCIENCE 16 (1981) 983–993

Preparation and properties of cast aluminium–ceramic particle composites

M. K. SURAPPA*, P. K. ROHATGI*
Regional Research Laboratory, Trivandrum 695 019, India

A casting technique for preparing aluminium–alumina, aluminium–illite and aluminium–silicon carbide particle composites has been developed. The method essentially consists of stirring uncoated but suitably heat-treated ceramic particles of sizes varying from 10 to 200 μm in molten aluminium alloys (above their liquidus temperature) using the vortex method of dispersion of particles, followed by casting of the composite melts. Recoveries and microscopic distribution of variously pretreated ceramic particles in the castings have been reported. Mechanical properties and wear of these composites have been investigated. Ultimate tensile strength (UTS) and hardness of aluminium increased from 75.50 MN m^{-2} and 27 Brinell hardness number (BHN) to 93.15 MN m^{-2} and 37 BHN respectively due to additions of 3 wt% alumina particles of 100 μm size. As a contrast, the tensile strength of aluminium–11.8 wt% Si alloy decreased from 156.89 MN m^{-2} to 122.57 MN m^{-2} due to the addition of 3 wt% alumina particles of the same size. Adhesive wear rates of aluminium, aluminium–11.8 wt% Si and aluminium–16 wt% Si alloys decreased from 3.62×10^{-8}, 1.75×10^{-8} and 1.59×10^{-8} $cm^3 cm^{-1}$ to 2.0×10^{-8}, 0.87×10^{-8} and 0.70×10^{-8} $cm^3 cm^{-1}$, respectively, due to the additions of 3 wt% alumina particles.

1. Introduction

Metal–ceramic particle composites have been recognized as candidate materials for wear resistant and bearing applications. In addition, they could present the means of conserving scarce metals by filling them with abundantly available ceramic particles. Among metal–ceramic particle composites, aluminium–graphite and aluminium–alumina particle composites can possess improved wear resistance, high-temperature hardness and strength, and may be used for several applications. It is reported that the addition of 1% alumina (7 μm particle size) in an aluminium alloy can lead to increased hardness and a four-fold increase in strength at 350° C [1]. Hypereutectic aluminium–silicon alloy containing alumina and zircon (33 to 240 μm particle size) have been used in automobile engines [2]. However, until recently aluminium–ceramic particle composites were generally made by conventional powder metallurgy methods. Only recently have attempts been made to prepare these composites by liquid metallurgy techniques (where the particles are introduced into the melt prior to solidification). The major difficulties in fabricating aluminium–ceramic particle composites by melt metallurgy techniques are: (1) Absence of wetting between molten aluminium and ceramic particles (oxides and carbides) at temperatures used in conventional foundry practice. The lack of wetting leads to rejection of the ceramic particles when they are added to the melt. (2) Segregation of dispersed particles in the melt and in the solidified castings due to density differences between aluminium and ceramic particles.

Several approaches have been employed to improve the wettability between liquid aluminium and ceramic particles. Badia [3] used nickel coating on the alumina particles to improve wetting between ceramic particles and liquid aluminium. Addition of surface active elements such as magnesium in aluminium alloy melt just prior to the introduction of the particles has been

*Formerly with the Department of Mechanical Engineering, Indian Institute of Science, Bangalore 560 012, India.

0022–2461/81/040983–11$03.10/0

TABLE I As-supplied composition of matrix alloys

Alloy	Metal (wt %)					
	Cu	Mg	Si	Fe	Mn	Others
Al	0.03	0.03	0.3	0.4	0.03	Al–99.5 min
Al–3 wt % Cu–4 wt % Si	3.0	0.1	4.0	–	–	–
Al–11.8 wt % Si	0.1	0.1	11.8	0.6	0.5	–
Al–16.0 wt % Si	0.1	0.1	16.0	0.6	0.5	–

employed by several workers [4–6] in the preparation of aluminium–graphite, aluminium–mica and aluminium–alumina particle composites. Flemings and Mehrabian [7] have been able to introduce and disperse insoluble refractory particles including aluminium oxide in aluminium alloys while the temperature of the alloys was maintained between their liquidus and solidus points. However, under their experimental conditions [7], they were unsuccessful in introducing alumina particles in liquid aluminium alloys above the liquidus temperature. Kaye [8] has reported the preparation of aluminium–ceramic (particle–fibre) composites in vacuum after cleaning the dispersoids by ion bombardment in vacuum at an elevated temperature.

The above work indicates that it would be desirable to develop a simpler technique of preparing aluminium–ceramic particle composites for the following reasons.

(1) Use of metal coated ceramic particles results in a change in the composition of matrix alloy which may not be desirable in certain cases. It also requires a source of metal coated ceramic particles.

(2) It is difficult to reproducibly control the addition of an innoculant like magnesium, and it also leads to small changes in the composition of the matrix. Also, magnesium additions lead to the formation of magnesium oxide on the periphery of the alumina particles which may be undesirable in certain applications [5, 6].

(3) The compocasting technique developed by Flemings and Mehrabian [7] requires specialized equipment to stir the alloys at temperatures between their liquidus and solidus points.

(4) Mixing of ceramic particles in liquid aluminium as reported by Kaye [8] requires cleaning of ceramic particles in vacuum by ion bombardment and preparation of the composite in vacuum.

In this paper a vortex technique will be reported for the introduction and dispersion of alumina, illite clay and silicon carbide particles in liquid aluminium and aluminium alloys, prior to casting the alloys as particle composites. The optimum conditions for the introduction and dispersion of these ceramic particles have been determined. In addition, hardness, tensile strength, ductility and wear resistance of aluminium–alumina and aluminium–silicon–alumina composites will be reported.

2. Experimental procedure

2.1. Materials used

Table I lists the as-supplied compositions of the base alloys (matrix materials) used in this study. γ-Al_2O_3 (density $2.4 \times 10^3 kg\,m^{-3}$) and -300 mesh α-SiC (density $3.1 \times 10^3 kg\,m^{-3}$) particles were obtained from Sarabhai Chemicals, India and Grindwell Norton, India, respectively, and -300 mesh illite clay (density $1.91 \times 10^3 kg\,m^{-3}$) was obtained from the Industrial Minerals and Chemicals Co., Bombay. Sieve analysis of aluminium oxide particles is shown in Table II. Theoretical densities of aluminium oxide, illite and silicon carbide are 3.8, 2.7 and $3.2 \times 10^3 kg\,m^{-3}$, respectively. Scanning electron micrographs of alumina, illite clay and silicon carbide particles are shown in Fig. 1a to c. The alumina particles are spheroidal whereas illite clay and silicon carbide particles are irregular in shape.

2.2. Dispersion of ceramic particles

The equipment used for dispersion of ceramic particles is similar to that reported elsewhere [9]. Heat treated particles were added to the melt through the sides of the vortex which was created by stirring the melt using a mechanical impeller.

TABLE II Sieve analysis of γ-Al_2O_3 particles

Mesh size	Size range (μm)	Content (wt %)
$-60, +100$	(149–280)	2
$-100, +140$	(105–149)	13
$-140, +200$	(74–105)	15
$-200, +240$	(63–74)	17
$-240, +300$	(53–63)	23.5
-300	53	29.5

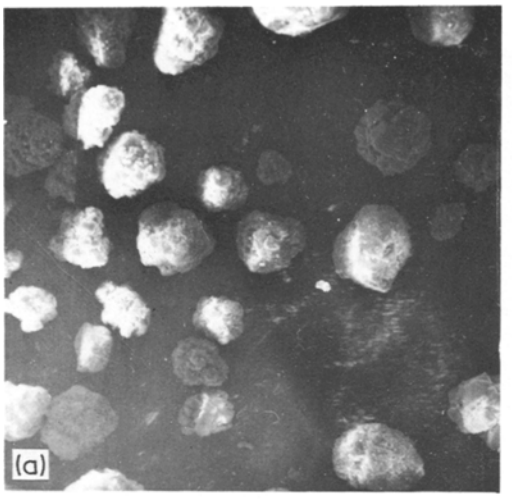

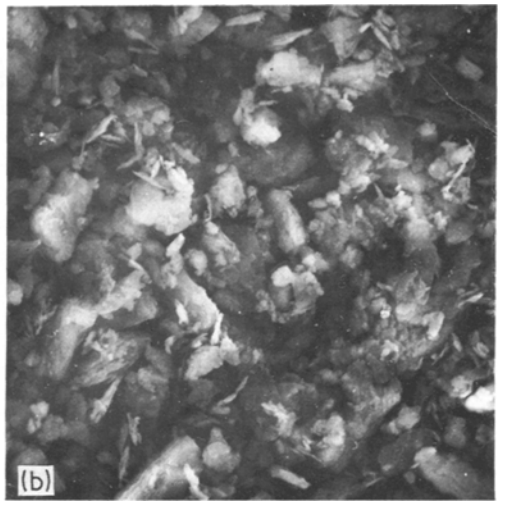

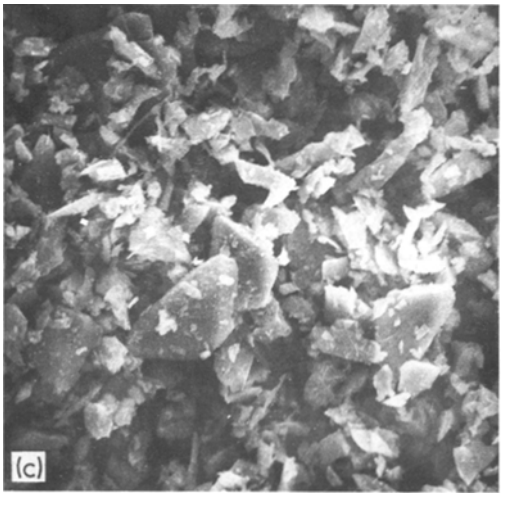

Figure 1 (a) Scanning electron micrograph of γ-Al_2O_3 particles (× 80), (b) scanning electron micrograph of illite clay particles (× 800) and (c) scanning electron micrograph of SiC particles (× 800).

The composite melt was stirred by hand with a graphite rod and poured into various cast iron moulds.

2.3. Centrifugal casting

Aluminium–11.8 wt % silicon alloy melts containing γ-alumina, illite clay and silicon carbide particles were poured, at 720° C, into rotating cast iron cylindrical moulds of 0.13 m internal diameter and 0.13 m height with a wall thickness of 0.02 m. The speed of rotation of the mould was 800 rpm just prior to pouring and while pouring it was increased to 1000 rpm in about 2 to 3 sec. The mould was spun for 1 min to ensure that solidification of the casting was completed. The solidified castings were sectioned to study the distribution of Al_2O_3 along longitudinal and transverse sections of the casting.

2.4. Microstructure

Specimens for microstructure examination were cut from permanent moulded cast Department of Trade and Industry (DTD) bars (0.025 m in diameter), polished on a series of SiC emery papers in water and finally on sylvet cloth using magnesium oxide as abrasive. Specimens were etched with 0.5% HF, and examined under an optical microscope.

2.5. Mechanical properties and wear resistance

Tests were conducted on specimens taken from the DTD test-bar casting. Only those test-bar castings with no visible voids or defects were used for mechanical testing.

2.5.1. Tensile testing

For tensile testing 22.5×10^{-3} m gauge length and 6.25×10^{-3} m diameter, specimens were used. Tensile properties were measured using an Instron testing machine at a cross-head speed of 0.005 m min^{-1}.

2.5.2. Hardness

Brinell hardness number (BHN) of the specimens was measured using a 5 mm diameter hardened steel ball indenter. A load of 250 kg was applied for 30 sec.

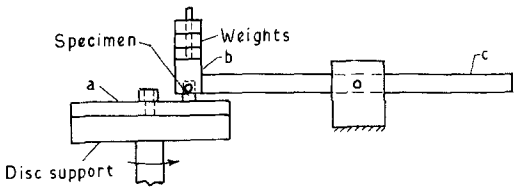

Figure 2 Schematic diagram of the wear apparatus (a) disc, (b) specimen holder and (c) arm.

2.5.3. Wear resistance

The apparatus used for evaluating the adhesive wear resistance is shown schematically in Fig. 2. A rotating steel disc (forged EN 24 steel of 57 Rc and ground to 0.3 μm CLA) was fixed onto a disc support which was directly connected to a 1.5 horsepower d.c. motor through a belt drive and driven at 850 rpm. A test sample (10^{-2} m in diameter x 10^{-2} m in length) was inserted into the specimen holder and tightened with the help of side screws. Test samples were cut from DTD test bars. A load of 2.0 kg was applied to the specimen. A fixed track diameter of 10.4×10^{-2} m was used in all the tests and all the tests were run for 10 min. However, every test was conducted on a fresh track by changing the disc. For these conditions the sliding distance and the sliding velocity were 2545 m and 4.24 m sec^{-1}, respectively. All the tests were carried out in air without lubrication and wear rates of Al–Al_2O_3, Al–11.8 wt% Si–Al_2O_3 and Al–16 wt% Si–Al_2O_3 composites were measured.

3. Results and discussion

3.1. Processing (composite fabrication)

Attempts by other researchers to incorporate uncoated particles and fibres such as alumina and silicon carbide into liquid aluminium alloys (above the liquidus temperature) have not been successful [5–7, 10–13]. This is due to the fact that contact angles of aluminium on alumina and silicon carbide are more than 90° at temperatures close to the melting point of aluminium. The uncoated ceramic particles are apparently not wetted by molten aluminium and are rejected by the melt. The presence of contaminants (adsorbed gas molecules, water molecules) on these ceramic particles, and the concomitant reduction in their surface energies, is presumably responsible for this non-wettability. However, in the present investigation it was possible to introduce suitably heat treated ceramic particles into molten aluminium alloys, and subsequently cast the melts into various shapes in metal moulds.

3.1.1. Al–Al_2O_3 system

The improved wetting between heat-treated aluminium oxide and molten aluminium around 800° C could possibly be due to a change in the surface characteristics and surface energy of aluminium oxide.

It has been reported that there is no marked change in the wetting angle between molten aluminium and alumina with a change in the crystal structure or crystal plane of alumina [14, 15]. Hence, the improved wetting between heat-treated aluminium oxide and molten aluminium is probably not due to a change in the overall crystal structure of aluminium oxide. In fact no apparent measurable change in the overall crystal structure of aluminium oxide was detected from the examination of Debye–Scherrer X-ray powder photographs of aluminium oxide particles before heat treatment, after heat treatment followed by cooling in air or after extraction from composite castings. Hence, the improved wetting between molten aluminium and heat-treated aluminium oxide observed in this investigation, is probably due to a change in the surface characteristics and surface energy of aluminium oxide. At room temperature, the surface of alumina is hydroxylated and the energy of the hydroxylated surface is 0.49 J m^{-2} less than the surface energy of the dehydroxylated surface [16]. Heating aluminium oxide particles to high temperatures ($\approx$ 900° C) will lead to dehydroxylation and the surface energy increases with dehydroxylation [14]. In this investigation, heat-treated alumina particles were probably wetted by molten aluminium around 800° C because of the increase in the surface energy of alumina. Brennan and Pask [17] have also reported a marked change in the contact angle between liquid aluminium and α-alumina as a result of heat treatment of the latter (Fig. 3). In their experiments heat treatment consisted of heating alumina in vacuum at 1300° C just prior to sessile drop experiments. Decrease in contact angle after heat treatment has been attributed to the formation of HTH surface (oxygen deficient surface of some unknown thickness containing some AlO in a spinel-type structure). Similar results have been reported [18] on the contact angle between Au–31 at% Si alloy and heat-treated α-Al_2O_3. These results suggest that apparently the heat treatment

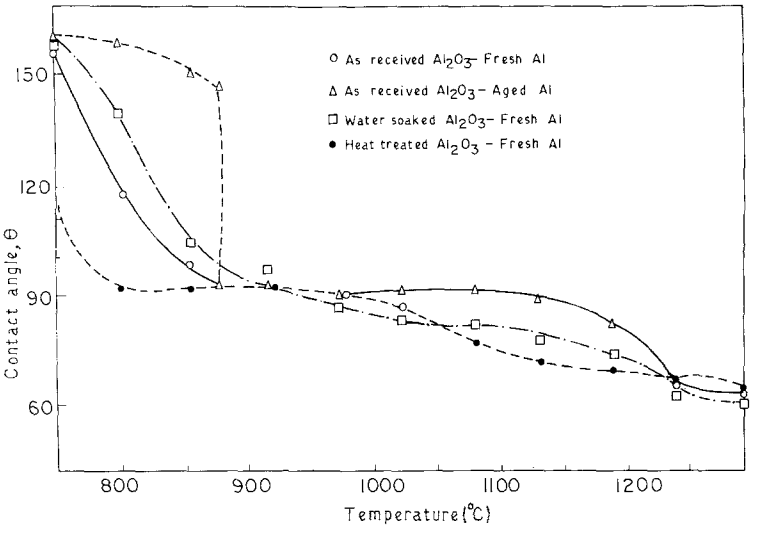

Figure 3 Change in contact angle with temperature for the system $Al–Al_2O_3$.

of alumina in the present investigation has also improved the wetting with aluminium melts thereby facilitating the introduction of alumina particles in to aluminium melts.

3.1.2. Al–illite system

Relatively little data are available about the wetting between molten aluminium and illite clay. The contact angle of aluminium on illite is, however, expected to be more than 90° [19]. In this investigation, as in the case of aluminium oxide, it was possible to disperse only the heat-treated illite particles in molten aluminium. As-received and unheat-treated particles were rejected by the melts.

3.1.3. Al–silicon carbide system

The wetting angle between molten aluminium and silicon carbide decreases with increasing temperature: it is 154° at the melting point of aluminium and 40° at 1100° C. In the present investigation it was possible to disperse heat-treated SiC particles in molten aluminium and prepare cast aluminium–silicon carbide particle composites where as-received SiC particles which are not heat treated were rejected by the melt.

3.2. Factors affecting the introduction and dispersion of ceramic particles in molten aluminium and aluminium alloys

The process variables affecting the dispersion of alumina, illite clay and silicon carbide particles in aluminium–11.8 wt % Si alloy melt are: (i) temperature and time of heat treatment of ceramic particles; (ii) particle size and shape; (iii) temperature of the melt during introduction of ceramic particles; (iv) rate of addition of ceramic particles; (v) percentage of dispersoid and (vi) melt de-gassing.

3.2.1. Heat treatment temperature and time

It was found necessary to heat alumina, illite clay and silicon carbide paticles to a temperature of about 900° C in air for a period of 1 h prior to introduction. Influence of heat treatment temperatures and time on dispersability of alumina, illite clay and SiC in Al–11.8 wt % Si alloy melt are shown in Table III. Once the particles were heated appropriately, the particles were allowed to cool while they were removed from the furnace and dispersed in the melt within about 10 min. When particles which were not heat treated prior to addition were introduced into the melts they were visibly rejected by the melts. Similarly, particles which where heated even up to 700° C for 4 h could not be introduced into the melt. Silicon carbide and illite clay particles when heated to 900° C for periods of more than 1 h showed a tendency to agglomerate which resulted in decreased recoveries (Table III): hence, the time of heating was restricted to only 1 h.

3.2.2. Particle size and shape

Recoveries of ceramic particles (preheated to 900° C for 1 h) in solidified castings (in terms of wt % particles added to Al–11.8 wt % Si alloy melt) were found to be dependent on the size and shape of the dispersoid. In the case of alumina particle additions the recoveries were better (96%)

TABLE III Influence of pre-heat treatment temperature and time on recovery of ceramic particles dispersed in aluminium–11.8 wt % silicon alloy melt (temperature of the melt at the time of introduction was 780° C)

Dispersoid	Wt % added	Pre-heat treatment		Per cent dispersoid in the casting	Percentage recovery of particles ≙ in the composite	Percentage dispersoid in the casting / Percentage dispersoid added in the melt × 100
		Temperature (°C)	Time (h)			
200 μm Al_2O_3	3	300	24	Nil	Nil	
200 μm Al_2O_3	3	500	15	Nil	Nil	
200 μm Al_2O_3	3	700	4	Nil	Nil	
200 μm Al_2O_3	3	800	3	0.5	16	
200 μm Al_2O_3	3	900	0.5	2.1	70	
200 μm Al_2O_3	3	900	1	2.9	96	
200 μm Al_2O_3	3	900	2	2.9	96	
60 μm Al_2O_3	3	900	0.5	1.5	50	
60 μm Al_2O_3	3	900	1	2.5	83	
60 μm Al_2O_3	3	900	2	2.7	90	
60 μm Al_2O_3	3	900	3	2.7	90	
Less than 53 μm size illite clay	3	900	1	1.5	50	
Less than 53 μm size illite clay	3	900	2	0.3	10	
Less than 53 μm size silicon carbide	3	900	1	1.0	33	
Less than 53 μm size silicon carbide	3	900	2	2.0	66	

with the addition of 200 μm size particles compared with recoveries (83%) obtained with the addition of 60 μm size particles. Recoveries obtained with the additions of less than 53 μm size illite and less than 53 μm size flake SiC particles are 50 and 33%, respectively. In addition to finer size, surface characteristics are possibly responsible for the low recoveries obtained in the case of illite and SiC particles.

3.2.3. Temperature of the melt

The temperature of the melt (aluminium or aluminium–silicon alloy) just prior to the introduction of ceramic particles was maintained around 780° C. Higher temperatures, especially above 820° C, resulted in severe erosion of the impeller blades. Until the addition of particles was completed, care was taken to maintain the temperature of the melt above 740° C. Attempts to introduce particles when the melt temperatures were below 700° C led to rejection of particles.

3.2.4. Rate of addition

Alumina, illite clay and silicon carbide particles were added to the melt at rates of 0.03 to 0.04 kg min^{-1}. When particles were added at rates higher than these, the particles became agglomerated and this resulted in very low recoveries.

3.2.5. Percentage of dispersoid

Theoretically a maximum of 60 vol% (if the particles were spherical) and 49 vol% (if the particles were granular) of powder can be incorporated into liquid metal contained in a semi-infinite container [20]. Under the present experimental conditions it was possible to introduce a maximum of only 6% coarse alumina particles (200 μm). However, due to local segregation of particles in the melts, it was possible in a few cases to obtain (a) castings containing a greater percentage of dispersoid than the average percentage of dispersoid added to the melt, when several castings were poured from the melt, and (b) a part of the casting with a greater percentage of dispersoid than the average percentage added due to the segregation of particles after the melts were poured into the mould. Similarly it was possible to introduce a maximum of only 3% of silicon carbide and illite particles into the melt. These upper limits could, however, be due to the specific experimental conditions employed in the present study.

3.2.6. Melt de-gassing

Aluminium alloy melts were de-gassed either with hexachloroethane or with nitrogen prior to the addition of ceramic particles. De-gassing the melts with chlorine bearing gas or with hexachloro-

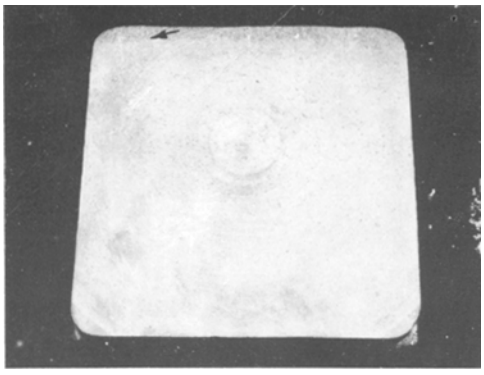

Figure 4 Photograph of machined surface of Al–11.8 wt % Si–2 wt % Al_2O_3 composite plate casting (0.15 m × 10.15 m × 0.025 m) showing the segregation of Al_2O_3 particles (indicated by the arrow) near the top (pouring temperature 740° C) (× 0.35).

ethane after the addition of particles lead to complete rejection of particles by the melt. After completing the addition of particles, the composite melts can be de-gassed with nitrogen.

In addition to the above process variables the chemical composition of the matrix also affects the recovery of dispersoids to some extent.

3.3. Distribution of ceramic particles in static and centrifugal castings

Machine cut surfaces of typical composite castings (machined to a depth of 1×10^{-3} m) made in this study are shown in Figs 4 to 6. Castings obtained by pouring the composite melts at 740° C into permanent moulds exhibited segregation of alumina particles near the top surface (Fig. 4) indicating that the particles floated upwards during pouring and solidification. On the other hand, in a similar composite casting made at a pouring temperature of 700° C the alumina particles were distributed homogeneously. Distribution of alumina particles on the section of such a casting is shown at a five-times magnification in Fig. 5. Photographs of typical longitudinal and transverse sections of centrifugally-cast cylinders of composition Al–11.8 wt % Si–2 wt % Al_2O_3, such as in

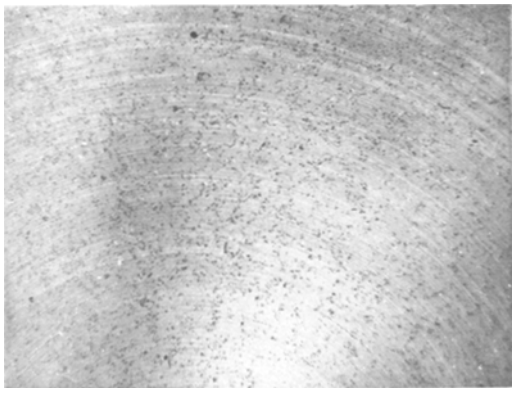

Figure 5 Photograph of machined surface of plate casting of composition of Al–11.8 wt % Si–2 wt % Al_2O_3 showing uniform distribution of alumina particles (pouring temperature 700° C) (× 4).

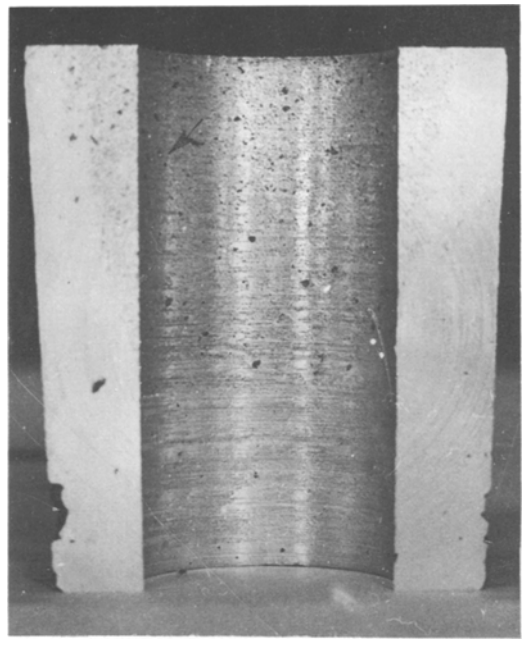

Figure 6 Photograph of longitudinal section of centrifugally cast cylinder of composition Al–11.8 wt % Si–2 wt % Al_2O_3 showing the segregation of alumina particles near the inner periphery and the top (indicated by the arrow) (× 0.54).

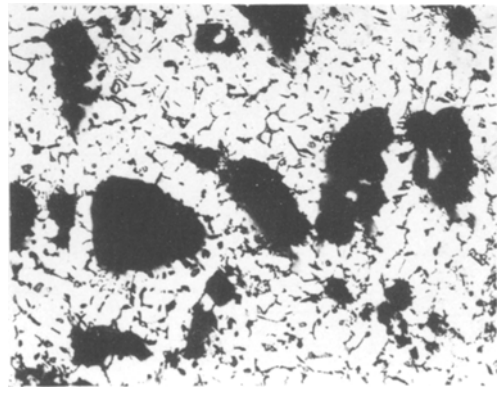

Figure 7 Microstructure of cast Al–3 wt % Cu–4 wt % Si–2 wt % SiC particle composites (× 200).

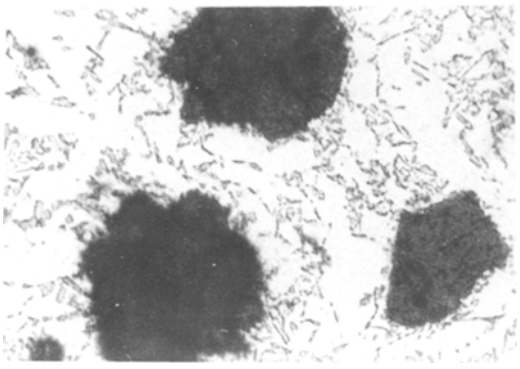

Figure 8 Microstructure of cast Al–11.8 wt % Si–4.5 wt % Al_2O_3 (× 400).

Fig. 6, indicate preferential segregation of alumina particles near the inner periphery and top of the castings. Similar kinds of segregation were observed in the case of illite and SiC particles.

3.3.1. Microstructure

In pure aluminium, dispersed alumina particles are present at grain boundaries and there is no marked change in the grain size due to the presence of dispersed Al_2O_3 particles. Microstructures of cast hypoeutectic aluminium–silicon alloy containing SiC particles also indicate (Fig. 7) preferential segregation of dispersed particles at interdendritic regions. This is attributed to the fact that during solidification of composite castings the dispersed ceramic particles are pushed by the growing aluminium dendrites into the last solidifying interdendrite regions due to the lower heat diffusivity of ceramic particles compared to aluminium melts [21]. In the present experiment the dendritic nature of the interface and the relatively large size of the particles would also increase the tendency for particle pushing. Microstructures of permanent mould cast Al–11.8 wt % Si–4.5 wt % Al_2O_3 composites shown in Fig. 8 illustrate the nucleation of eutectic silicon needles around dispersed Al_2O_3 particles. Elemental X-ray scanning of silicon for the composite clearly establishes segregation of silicon around dispersed Al_2O_3 particles (Fig. 9). Figs 10 and 11 show the microstructures of cast Al–16 wt % Si–4 wt % Al_2O_3 composite (0.086 m diameter and 0.15 m height cylinder) at a distance of 0.075 m and 0.08 m, respectively, from the bottom end of the casting. The casting is free from alumina particles due to their flotation during solidification up to a height of 0.078 m from the bottom end. Marked refinement of primary silicon is observed due to the presence of 4 wt % alumina particles. This observation is in agreement with the results of

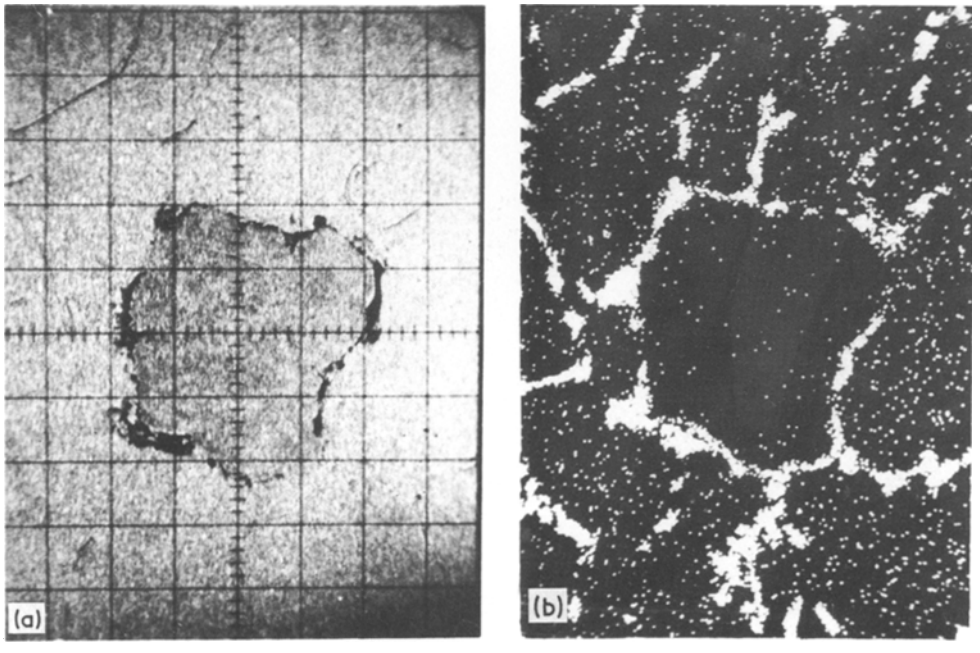

Figure 9 (a) SEM view of the region (secondary electron image) around dispersed Al_2O_3 (in Al–11.8 wt %Si–Al_2O_3 composite) (× 450) and (b) elemental silicon X-ray map around dispersed Al_2O_3 particles in Al–11.8 wt % Si–Al_2O_3 composite (× 500).

Figure 10 Microstructure of cast Al–16 wt % Si–4 wt % Al_2O_3 particle composite (specimen taken at a height of 0.075 m from the bttom end of 0.087 diameter and 0.15 m height casting) (× 200).

Figure 11 Microstructure of the same casting as Fig. 10 at a height of 0.8 m from the bottom and where alumina particles are present (× 200).

Cisse *et al.* [22]. However, they found that Al_2O_3 promotes nucleation of α-aluminium only when it is produced *in situ* by reduction of silver oxide by aluminium in the melt.

3.3.2. Mechanical properties

Ultimate tensile strength (UTS), hardness and percentage elongation of Al–Al_2O_3 and Al–11.8 wt % Si–Al_2O_3 composites are shown in Table IV. UTS and hardness of aluminium increased from 75.5 MN m^{-2} and 27 BHN to 93.15 MN m^{-2} and 37 BHN, respectively, due to the addition of 3 wt % Al_2O_3 particles of 100 μm size. The increased hardness of composites could be attributed to the relatively high hardness of Al_2O_3 compared with that of aluminium. The increased hardness and relatively large percentage elongation which may be accompanied by work hardening appears to be responsible for increased UTS of Al–Al_2O_3 composites. On the contrary, the tensile strength of Al–11.8 wt % Si alloy decreased from 156.89 to 122.57 MN m^{-2} due to the addition of 3 wt % Al_2O_3 of 100 μm particle size. However, the hardnesses of Al–11.8 wt % Si and Al–11.8 wt % Si–3 wt % Al_2O_3 composites are 55 and 63 BHN, respectively. These results are in agreement with those of Plate [23]. Plate also reports an increase in the UTS of aluminium and a decrease in the tensile strength of Al–12 wt % Si with the addition of alumina particles. However, the compressive strengths of Al and Al–11.8 wt % Si alloy increase with additions of alumina particles [24].

3.3.3. Wear resistance

Results of adhesive wear tests on Al–Al_2O_3, Al–11.8 wt % Si–Al_2O_3 and Al–16 wt % Si–Al_2O_3 composites are plotted graphically in Fig. 12. From Fig. 12 it is clear that (a) the adhesive wear rate of aluminium is higher than that of Al–11.8 wt % Si and Al–16 wt % Si alloys. The wear rate of Al–11.8 wt % Si alloy is higher than that of Al–16 wt % Si alloy. This observation is in agreement with the results of Shivanath *et al.* [25], indicating that the presence of hard dispersed silicon needles decreases the rate of wear, (b) the adhesive wear rate of aluminium and aluminium–silicon alloy decreases with additions of Al_2O_3

TABLE IV Mechanical properties of Al–Al_2O_3 particle (100 μm) and Al–11.8 wt % Si–Al_2O_3 particle (100 μm) composite

Composition	Hardness (BHN)	UTS (MN m^{-2})	Percentage Elongation
Al	27	75.50	37.5
Al–1 wt % Al_2O_3	31	80.40	34
Al–2 wt % Al_2O_3	35	86.29	23.4
Al–3 wt % Al_2O_3	37	93.15	18
Al–11.8 wt % Si	55	156.89	6
Al–11.8 wt % Si–1 wt % Al_2O_3	59	137.28	3.8
Al–11.8 wt % Si–2 wt % Al_2O_3	61	129.43	3.4
Al–11.8 wt % Si–3 wt % Al_2O_3	63	122.57	3
Al–11.8 wt % Si–4.5 wt % Al_2O_3	64	118.65	2.5

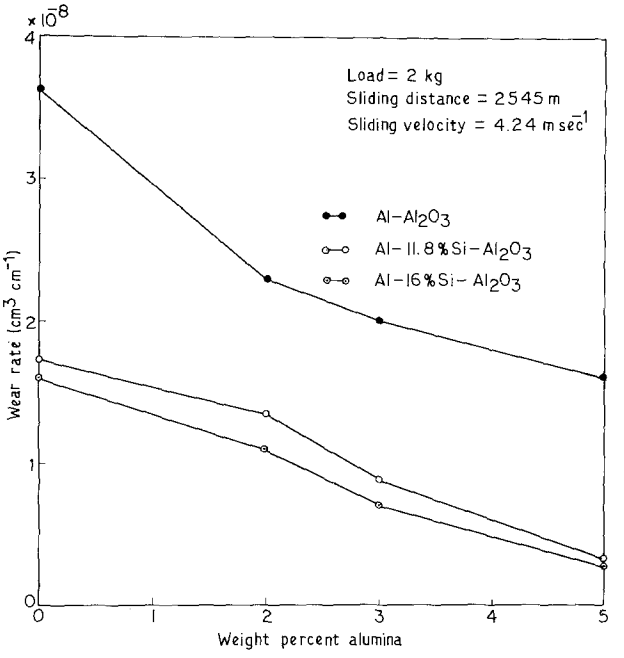

Figure 12 Wear rates of aluminium, aluminium–11.8 wt % Si and aluminium–16 wt % Si alloys containing different wt % alumina particles.

particles and (c) the adhesive wear rate of Al–5 wt % Al_2O_3 composite is lower than that of Al–11.8 wt % Si alloy under the present experimental conditions. The observed improvement in the wear resistance of Al–Al_2O_3 composites could be attributed to the presence of dispersed Al_2O_3 and increased hardness.

A typical scanning electron micrograph of a worn surface of Al–16 wt % Si–5 wt % Al_2O_3 composite is shown in Fig. 13. It indicates that alumina particles are not pulled out during the wear process, which is indicative of a good wear resistant material.

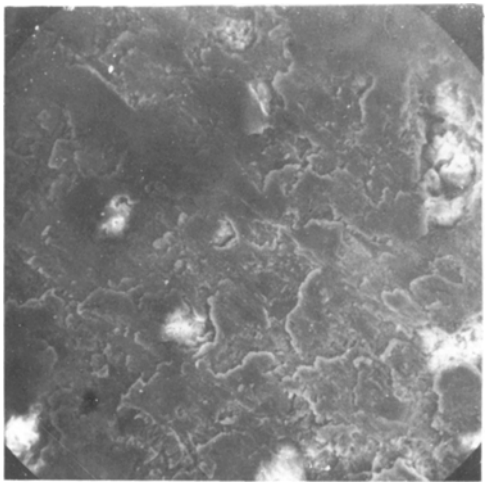

Figure 13 SEM view of worn surface of cast Al–16 wt % Si–5 wt % Al_2O_3 (100 μm) composite on En 31 steel (× 70).

4. Conclusions

(1) Cast aluminium–alumina, aluminium–illite and aluminium–silicon carbide composites can be prepared by introducing suitably heat treated ceramic particles (alumina, illite and silicon carbide) into molten aluminium alloys using the vortex method of dispersion of powders followed by casting of the composite melts into suitable moulds.

(2) Preheating of the particles for a period of 60 min at 900° C prior to their addition to the melt aids in the introduction of these particles into the melt.

(3) Melts of aluminium alloys containing suspended alumina, silicon carbide and illite particles can be permanent mould cast in a variety of shapes with a macroscopially uniform distribution of ceramic particles. On a microscopic scale these ceramic particles are generally present at the grain boundaries in pure aluminium and in the last frozen interdendrite regions in hypo-eutectic aluminium alloys. In Al–16 wt % Si–ceramic particles composites, the primary silicon cuboids are frequently nucleated preferentially on dispersed particles of alumina, illite clay and silicon carbide.

(4) UTS and hardness of aluminium increases from 75.50 MN m^{-2} and 27 BHN to

93.15 MN m^{-2} and 37 BHN, respectively, due to the addition of 3 wt % alumina particles of 100 μm size.

(5) The adhesive wear of aluminium decreases from 3.62×10^{-8} to 2.0×10^{-8} $cm^3 cm^{-1}$ due to the addition of 3 wt % alumina particles.

References

1. G. L. TSAREV, I. S. LITMANOVICH and T. A. RYABKO, *Vesti Akab. Nauk B. SSR, Ser, Fix-Tech, Nauk* **1** (1976) 28.
2. R. N. SANDERS and A. R. VALDO, Eyhyl Corporation, Aluminium–silicon composite, US Patent, 3961, 945.
3. F. A. BADIA, *American Foundrymen's Society Trans.* **79** (1971) 347.
4. V. G. GORBUNOV, U. D. PARSHIN and V. V. PANIN, "Russian Casting Production", August 1974. p. 348.
5. B. C. PAI, S. RAY, K. V. PRABHAKER and P. K. ROHATGI, *Mater. Sci. Eng.* **24** (1976) 31.
6. DEONATH, R. T. BHAT and P. K. ROHATGI, *J. Mater. Sci.* **15** (1980) 1241.
7. M. C. FLEMINGS and R. MEHRABIAN, *Metal. Trans.* **5** (1974) 1899.
8. S. KAYE, *J. Vac. Sci. Tech.* **11** (1974) 1114.
9. M. K. SURAPPA and P. K. ROHATGI, *Met. Tech.* **5** (1978) 358.
10. F. A. BADIA and P. K. ROHATGI, *AFS Trans.* 77 (1969) 402.
11. A. M. PATTON, *J. Inst. Met.* **100** (1972) 197.
12. C. G. LEVI, G. S. ABBASCHAIAN and R. MEHRABIAN, *Metall. Trans.* **9A** (1978) 697.
13. P. K. ROHATGI, B. C. PAI and P. C. PANDA, *J. Mater. Sci.* **14** (1979) 2277.
14. S. K. RHEE, *J. Amer. Ceram. Soc.* **55** (1972) 300.
15. W. KOHLER, *Aluminium* 7 (1975) 443.
16. D. HARDIS and N. J. PETCH, *Proc. Brit. Ceram. Soc.* **5** (1965) 85.
17. J. BRENNAN and J. A. PASK, *J. Amer. Ceram. Soc.* **51** (1968) 569.
18. C. MARUMO and J. A. PASK, *ibid.* **60** (1977) 276.
19. J. A. PASK, Private Communication, 1978.
20. W. H. STEURER and S. KAYE, Preparation of composite Materials in Space, General Dynamics (Convair Division) California, Report No. GDCA-DBG 73-001 Jan. 1973.
21. M. K. SURAPPA and P. K. ROHATGI, *J. Mater. Sci.* **16** (1981) 562.
22. J. CISSE, G. F. BOLLING and H. W. KERR, *Metall. Trans.* **68** (1975) 195.
23. H. PLATE, Ph.D thesis, Techniechen Hochschule, Auchen, 1971.
24. M. K. SURAPPA, Ph.D thesis, Indian Institute of Science, 1979.
25. R. SHIVNATH, P. K. SENGUPTA and T. S. EYRE, *British Foundrymen* **70** (1977) 349.

Received 30 April and accepted 10 September 1980.